Accepted Manuscript


# DTA0100, dual topoisomerase II and microtubule inhibitor, evades paclitaxel resistance in P-glycoprotein overexpressing cancer cells

Ana Podolski-Renić, Jasna Banković, Jelena Dinić, Carla Ríos-Luci, Miguel X. Fernandes, Nuria Ortega, Nataša Kovačević-Grujičić, Víctor S. Martín, José M. Padrón, Milica Pešić

PII: S0928-0987(17)30239-7
DOI: doi: 10.1016/j.ejps.2017.05.011
Reference: PHASCI 4025

To appear in: *European Journal of Pharmaceutical Sciences*

Received date: 6 December 2016
Revised date: 29 March 2017
Accepted date: 5 May 2017

Please cite this article as: Ana Podolski-Renić, Jasna Banković, Jelena Dinić, Carla Ríos-Luci, Miguel X. Fernandes, Nuria Ortega, Nataša Kovačević-Grujičić, Víctor S. Martín, José M. Padrón, Milica Pešić , DTA0100, dual topoisomerase II and microtubule inhibitor, evades paclitaxel resistance in P-glycoprotein overexpressing cancer cells, *European Journal of Pharmaceutical Sciences* (2017), doi: 10.1016/j.ejps.2017.05.011

This is a PDF file of an unedited manuscript that has been accepted for publication. As a service to our customers we are providing this early version of the manuscript. The manuscript will undergo copyediting, typesetting, and review of the resulting proof before it is published in its final form. Please note that during the production process errors may be discovered which could affect the content, and all legal disclaimers that apply to the journal pertain.

ACCEPTED MANUSCRIPT

# DTA0100, dual Topoisomerase II and microtubule inhibitor, evades paclitaxel resistance in P-glycoprotein overexpressing cancer cells

Ana Podolski-Renić[a,*], Jasna Banković[a], Jelena Dinić[a], Carla Ríos-Luci[b], Miguel X. Fernandes[b], Nuria Ortega[b], Nataša Kovačević-Grujičić[c], Víctor S. Martín[b], José M. Padrón[b], and Milica Pešić[a]

[a] Institute for Biological Research „Siniša Stanković“, University of Belgrade, Despota Stefana 142, 11060 Belgrade, Serbia

[b] BioLab, Instituto Universitario de Bio-Organica "Antonio Gonzalez" (IUBO-AG), Centro de Investigaciones Biomédicas de Canarias (CIBICAN), Universidad de La Laguna, Avda. Astrofisico Francisco Sánchez 2, 38206 La Laguna, Tenerife, Spain

[c] Institute of Molecular Genetics and Genetic Engineering, University of Belgrade, Vojvode Stepe 444a, PO BOX 23, 11010 Belgrade, Serbia

[*]Corresponding author:

Email: ana.podolski@ibiss.bg.ac.rs, phone: +381 11 2078 406, fax: +381 11 2761 433

ACCEPTED MANUSCRIPT

## Abstract

The efficacy of microtubule targeting agents in cancer treatment has been compromised by the development of drug resistance that may involve both, P-glycoprotein overexpression and the changes in β-tubulin isoforms' expression. The anti-Topoisomerase II activity of methyl 4-((E)-2-(methoxycarbonyl)vinyloxy)oct-2-ynoate (DTA0100) was recently reported. Herein, we further evaluated this propargylic enol ether derivative and found that it exerts inhibitory effect on tubulin polymerization by binding to colchicine binding site. DTA0100 mitotic arrest properties were investigated in two multi-drug resistant cancer cell lines with P-glycoprotein overexpression (colorectal carcinoma and glioblastoma). The sensitivity of multi-drug resistant cancer cell lines to DTA0100 was not significantly changed in contrast to microtubule targeting agents such as paclitaxel, vinblastine and colchicine. DTA0100 clearly induced microtubule depolymerization, leading to disturbance of cell cycle kinetics and subsequent apoptosis. The fine-tuning in β-tubulin isoforms expression observed in multi-drug resistant cancer cells may influence the efficacy of DTA0100. Importantly, DTA0100 blocked the P-glycoprotein function in both multi-drug resistant cancer cell lines without inducing the increase in P-glycoprotein expression. Therefore, DTA0100 acting as dual inhibitor of Topoisomerase II and microtubule formation could be considered as multi-potent anticancer agent. Besides, it is able to overcome the problem of drug resistance that emerges in the therapeutic approaches with either Topoisomerase II or microtubule targeting agents.

**Key words:** β-tubulin; colchicine; microtubule targeting agents; multi-drug resistance; paclitaxel; P-glycoprotein

ACCEPTED MANUSCRIPT

## 1. Introduction

Microtubule targeting agents and Topoisomerase II inhibitors are important anticancer drugs that have been widely used in cancer therapy. Microtubule targeting agents disrupt microtubule dynamics by binding to the β-tubulin subunit on α/β-dimers, inducing mitotic arrest and cell death (Jordan and Wilson, 2004). Clinically important microtubule targeting agents can be subdivided into two broad groups, microtubule stabilizing agents (taxanes and epothilones) and microtubule destabilizing agents (colchicine and *Vinca* alkaloids) (Jordan and Wilson, 2004). Topoisomerase II inhibitors stabilize topoisomerase II - DNA complex in which the Topoisomerase II enzyme is covalently linked to the cleaved two strands of the DNA. These inhibitors enhance the level of DNA double-strand breaks, thereby activating DNA damage response, eventually leading to cell cycle arrest either in G1, S, or G2/M phase, and apoptosis (Bailly, 2012). The most important subclasses of topoisomerase II inhibitors in the clinics are epipodophyllotoxins and anthracyclines (Hande, 2008).

Microtubule targeting agents and Topoisomerase II inhibitors are frequently used in combination due to their different mechanisms of action. However, changes in drug binding sites on microtubule or Topoisomerase II could also confer drug resistance by reducing the effective drug binding (Ganapathi and Ganapathi, 2013; McGrogan et al., 2008). In addition, both types of inhibitors are substrates for P-glycoprotein, a membrane transporter, which overexpression is responsible for the development of multi-drug resistance (Sharom, 2008). P-glycoprotein belongs to the large ATP-Binding Cassette transporter family (Riordan and Ling, 1985) and acts as an efflux pump for various hydrophobic anticancer drugs, such as anthracyclines, Vinca alkaloids,

ACCEPTED MANUSCRIPT

taxanes, epipodophyllotoxins and colchicine leading to changed pharmacodynamics of these drugs (Bikadi et al., 2011; Wang et al., 2005).

Finding a new agent that may influence both Topoisomerase II activity and microtubule dynamics with a capacity to overcome the aforementioned obstacles for successful therapy outcome is challenging.

Recently, methyl 4-((*E*)-2-(methoxycarbonyl)vinyloxy)oct-2-ynoate (DTA0100) (Fig. 1A) was selected from a small and structure-focused library of propargylic enol ethers (León, et al., 2010). Docking studies of this compound against Topoisomerase II suggested that DTA0100 act as Topoisomerase II catalytic inhibitor (Silveira-Dortaet al., 2013). This compound induced cell cycle arrest in G2/M phase in various human cancer cell lines (León, et al., 2010). It is known that either Topoisomerase II inhibitors or microtubule targeting agents can cause cell cycle arrest at G2/M phase.

Therefore, in this study, we further explored mitotic arrest properties of DTA0100. To that end, we employed two pairs of multi-drug resistant and their corresponding sensitive human cancer cell lines - colorectal carcinoma and glioblastoma (Podolski-Renić et al., 2011). Both multi-drug resistant cancer cell lines, established after continuous exposure to microtubule stabilizing agent paclitaxel, showed overexpression of P-glycoprotein. Our findings suggest that besides inhibition of Topoisomerase II that was documented previously (Silveira-Dorta et al., 2013), DTA0100 also acts as a microtubule targeting agent which pharmacokinetics is not changed in the presence of P-glycoprotein.

ACCEPTED MANUSCRIPT

## 2. Materials and methods

### 2.1. Synthesis of dansyl-DTA0100

DTA0100 was selected from a small library of propargylic enol ethers (León, et al., 2010). DTA0100 was tagged with dansyl to generate fluorescent labelled DTA0100 (dansyl-DTA0100). Synthetic procedures and compound characterization data are given in Supplementary material. Synthesis of dansyl-DTA0100 is represented in Supplemental Fig. 1. Supplemental Fig. 2 represents $^{1}H$ and $^{13}C$ NMR spectra for compound 2 in $CDCl_3$. Supplemental Fig. 3 represents $^{1}H$ and $^{13}C$ NMR spectra for compound 3 in $CDCl_3$. Supplemental Fig. 4 represents $^{1}H$ and $^{13}C$ NMR spectra for compound 4 in $CDCl_3$. Supplemental Fig. 5 $^{1}H$ and $^{13}C$ NMR spectra for compound 5 in $CDCl_3$.

### 2.2. Drugs

Paclitaxel and vinblastine were purchased from Sigma-Aldrich Chemie GmbH, Germany. Colchicine was generous gift from the Department of Cytology, Institute for Biological Research, Belgrade, Serbia. DTA0100 and dansyl-DTA0100were dissolved in dimethyl sulfoxide (40 mM aliquots) and kept at -20 °C until use. Paclitaxel was diluted in absolute ethanol and 1 mM aliquots were stored at -20 $^{o}$C. Colchicine was diluted in sterile water and kept at 4 °C. Vinblastine was diluted in sterile water and 1mM aliquots were thawed from -20 $^{o}$C before use. Before treatment, all drugs were freshly diluted in sterile water.

### 2.3. Chemicals

ACCEPTED MANUSCRIPT

RPMI 1640 medium, Minimum Essential Medium, fetal bovine serum, antibiotic-antimycotic solution, penicilin-streptomicin solution, L-glutamine and trypsin/EDTA were purchased from Bioind, Beit Haemek, Israel. Rhodamine 123, sulforhodamine Band β-tubulin antibody were obtained from Sigma-Aldrich Chemie Gmbh, Germany. Secondary antibody Alexa Fluor 488 goat anti-rabbit IgG (H+L) was obtained from Cell Signaling Technology Inc. (Danvers, Massachusetts, USA). Annexin-V-FITC (AV) apoptosis detection kit was purchased from Abcam, Cambridge, UK. Propidium iodide (PI) was obtained from Roche Applied Science, Basel, Switzerland, while ribonuclease A was purchased from Invitrogen Life Technologies, USA.

### 2.4. *In vitro* tubulin polymerization assay

Microtubule-turbidity assay was carried out using the tubulin polymerization kit (Cytoskeleton Inc, Denver, USA). The assay was performed according to the manufacturer's recommended procedure. Briefly, each experimental compound (final concentration of 10 μM) was incubated with GTP-supplemented tubulin supernatant (3 mg/mL) in a 96-well plate at 37 °C. Polymerization reactions were followed by absorbance at 340 nm for 30 min using a BioTek's PowerWave XS Absorbance Microplate Reader every 20 seconds.

### 2.5. Molecular docking study

The crystal structure of the colchicine pocket from α,β-tubulin (PDB ID:3E22) was utilized as template for docking studies using the program AutoDock Vina (The Scripps Research Institute, La Jolla, USA). Initial structures were drawn and minimized using AM1 semi-empirical method, with a gradient energy minimization method until the energy change between steps was lower

ACCEPTED MANUSCRIPT

than 0.01 kcal/mol (Hyperchem, Hypercube, USA). The algorithm used was the Polak-Ribiere (conjugate gradient). The best solution (based on docking score) was retained for further analysis. PyMol v1.5 (Shrödinger Inc, Portland, USA) was used for visualization and identification of residues in the binding pocket.

### 2.6. Cells

DLD1 (human colorectal carcinoma) and U87 (human glioblastoma) cell lines were purchased from the American Type Culture Collection, Rockville, MD. DLD1-TxR and U87-TxR cells were selected by continuous exposure to stepwise increasing concentrations of paclitaxel from DLD1 and U87 cells, respectively (Podolski-Renić et al., 2011).

### 2.7. Sulforhodamine B assay

Cell viability was assessed by the sulforhodamine B assay according to the previously described procedure (Podolski-Renić et al., 2011). Cells grown in 25 $cm^2$ tissue flasks were trypsinized, seeded into flat-bottomed 96-well tissue culture plates (1,000 cells/well for DLD1 and DLD1-TxR, 4,000 cells/well for U87 and U87-TxR) and incubated over-night. Then, the cells were treated 72 h with increasing concentrations of DTA0100, colchicine, paclitaxel and vinblastine. Growth inhibition (GI)50 value was defined as a concentration of each drug that inhibited cell growth by 50%. GI50 was calculated by nonlinear regression analysis using GraphPad Prism 6.

### 2.8. Cell death detection

ACCEPTED MANUSCRIPT

The percentages of apoptotic, necrotic and viable cells were determined by AV/PI labeling. All cell lines were seeded in adherent 6-well plates (30,000 cells/well for DLD1 and DLD1-TxR, 200,000 cells/well for U87 and U87-TxR) and incubated overnight. Then, DLD1 and DLD1-TxR cells were subjected to treatment with 0.9 µM DTA0100, while U87 and U87-TxR cells were treated with 7.5 µM DTA0100. Paclitaxel and colchicine were used as positive controls. After 72 h, total (attached and floating) cells were collected. AV/PI staining was performed according to the manufacturer's instructions and cells were analyzed within 1 h by flow-cytometry.

**2.9. Flow-cytometric analysis of cell cycle distribution**

DLD1, DLD1-TxR, U87 and U87-TxR cells were plated in 25 $cm^2$ flasks and incubated overnight. The effects of DTA0100 on cell cycle distribution were studied after 72 h. Briefly, the attached and floating cells were trypsinized and collected by centrifugation, washed in phosphate buffered saline (PBS) and fixed in 70% ethanol for 48 h at -20 °C. After fixation, the cells were washed in PBS and pretreated with 133 µg/ml of ribonuclease A at 37 °C for 15 min. Then, PI was added to final concentration 17 µg/ml. After 30 min flow-cytometric analysis was performed on the FACSCalibur flow-cytometer (Becton Dickinson, United Kingdom). A minimum of 10,000 events were collected for each experimental sample. Cell cycle distribution was determined automatically in Mod-FIT (Verity Software House, Inc). The validity of the data analysis model was verified using the R.C.S. value (reduced Chi-square, R.C.S. < 15%).

**2.10. Fluorescence microscopy**

ACCEPTED MANUSCRIPT

To evaluate the effect of DTA0100 on microtubules, multi-drug resistant cells and their sensitive counterparts were labeled with β-tubulin antibody. DLD1, DLD1-TxR, U87 and U87-TxR cells were seeded in 4-chamber slides (Nunc, Naperville, USA) and allowed to grow overnight. Prior to immunostaining, DLD1, DLD1-TxR and U87 cells were subjected to single treatment with 5 μM DTA0100, while U87-TxR cells were treated with 10 μM DTA0100 for 24 h at 37 ºC. Colchicine and paclitaxel were used as positive controls. Sensitive cells were treated with 50 nM colchicine and 100 nM paclitaxel, while resistant cells were treated with 300 nM colchicine and 2 μM paclitaxel. After treatment, cells were washed in PBS, fixed in 4% paraformaldehyde and blocked with 2% bovine serum albumin in 0.3% Triton X-100 in PBS for 1 h at room temperature. Rabbit β-tubulin antibody was applied at 1:250 dilution in 0.3% Triton X-100 in PBS and cells were incubated overnight at 4 ºC. After washing with PBS, secondary antibody Alexa Fluor 488 goat anti-rabbit IgG (H+L) was applied at 1:1,000 dilution in 0.3% Triton X-100 in PBS for 2 h at room temperature. Nuclei were counterstained with Hoechst 33342 for 15 min at room temperature and cells were mounted in Mowiol. The cells were examined under Zeiss Axiovert inverted fluorescent microscope (Carl Zeiss Foundation, Germany) equipped with AxioVision 4.8 Software. To quantify microtubule depolimerization, mean fluorescence and background readings in aquired images were measured using ImageJ software v1.50i (U.S. National Institutes of Health, Bethesda, MD, USA). Corrected total cellular fluorescence (CTCF) was calculated as previously described (McCloy et al., 2014).

**2.11. Immunostaining, confocal microscopy and image analysis**

U87-TxR cells were seeded in 4-chamber slides and allowed to grow overnight. Cells were than treated with 30 μM dansyl-DTA0100 for 1 h at 37 ºC. After treatment, cells were

ACCEPTED MANUSCRIPT

fixed, blocked and labeled with β-tubulin antibody as described earlier. Images were acquired on a Leica TSC SP8 confocal microscope (Leica Microsystems) equipped with 488/552 nm lasers using 63/1.4 NA oil immersion lens. Colocalization analysis was performed in ImageJ software (NIH, USA) and the degree of colocalization between β-tubulin and DTA0100 was measured using the Pearson correlation coefficient (PCC). PCC measures the strength of a linear relationship between fluorescent intensities from the two images and produces values ranging from 1 (perfect positive correlation) to -1 (perfect inverse correlation), with 0 representing a random distribution (Manders et al., 1992; Manders et al., 1993).

**2.12. RNA extraction and RT-PCR reaction**

Total RNA was isolated from DLD1, DLD1-TxR, U87 and U87-TxR cell lines using Trizol® reagent (Invitrogen Life Technologies, USA). Reverse transcription reactions were performed with a high-capacity cDNA reverse transcription kit (Applied Biosystems). Polymerase chain reactions (PCR) were performed with primers specific for βI- and βIVb-tubulin (Leandro-García et al., 2010), βII- and βIII-tubulin (Shalli et al., 2005) and Topoisomerase IIα (Beck et al., 1999). Either gapdh (Wong et al., 1994) or β-actin (Ponte et al., 1984) were used as an internal control and were coamplified with the gene of interest in all PCR reactions. The PCR reactions were performed on a GeneAmp® PCR System 9700 (Applied Biosystems) under the following conditions: initial denaturation at 94 ºC for 5 min, 28 cycles at 94 ºC for 15 s, 56 ºC for 30 s, 72 ºC for 30 s, and at 4 ºC indefinitely. When PCR was performed to determine the expression of the Topoisomerase IIα, 28 cycles were decreased to 26 cycles. The gapdh primers were used at ratio of 1:5, while β-actin primers were used at ratio of 1:2 to gene of interest. The PCR products were separated on 2% agarose gels stained with ethidium

ACCEPTED MANUSCRIPT

bromide. MultiAnalyst/PC Software Image Analysis (Bio-Rad Gel Doc 1000) was employed for densitometry analysis.

### 2.13. DNA sequencing

Genomic DNA was extracted from cell culture samples using the GeneJET$^{TM}$ Genomic DNA Purification kit (Fermentas, Thermo Fisher Scientific, USA). The exons of the *βI-tubulin* gene (1-3) were amplified by PCR and screened for mutations by DNA sequencing. Primers for *βI-tubulin* gene were previously described in Ferguson et al. (2005). PCR conditions for all amplicons were 95 ºC for 5 min, 35 cycles at 95 ºC for 30 s, 60 ºC for 30 s, 72 ºC for 30 s, and completed by incubation at 72 ºC for 7 minutes with a final hold at 4 ºC. Amplified exons of *βI-tubulin* gene were subjected to DNA sequencing. Sequences were determined with Applied Biosystems Incorporated (ABI) dye terminator sequencing kits according to the manufacturer's specifications on an ABI Prism 3130 automated sequencer (Applied Biosystems, Foster City, CA, USA). Sequencing was carried out in both directions. The obtained sequences were analyzed and compared with wild type *βI-tubulin* sequence using BLAST software in the NCBI GenBank database.

### 2.14. Rhodamine 123 accumulation assay

Rhodamine 123 accumulation was analyzed by flow-cytometry as previously described (Podolski-Renić et al., 2011). Studies were carried out with DTA0100 and colchicine on DLD1, DLD1-TxR, U87 and U87-TxR cells. In simultaneous treatment with 5 μM rhodamine 123, multi-drug resistant cancer cells were treated with 1, 5 and 10 μM DTA0100 and 10 μM colchicine and incubated at 37°C in 5% $CO_2$ for 30 min. In pretreatment administration, multi-

ACCEPTED MANUSCRIPT

drug resistant cancer cells were pretreated with 10 μM DTA0100 for 0, 30 and 60 min before administration of 5 μM rhodamine 123 that lasted additional 30 min. All the time, DTA0100 was present in the medium.

### 2.15. Flow-cytometric analysis of P-glycoprotein expression

Flow-cytometry was used to measure P-glycoprotein expression level in DLD1, DLD1-TxR, U87 and U87-TxR cells. All cell lines were seeded in adherent 6-well plates and incubated overnight. Then, DLD1-TxR cells were treated with 0.9 μM DTA0100, while U87-TxR cells were treated with 7.5 μM DTA0100. After 72 h, cells were collected by trypsinization, washed in ice-cold PBS, and then directly immuno-stained by FITC-conjugated anti-P-glycoprotein antibody according to the manufacturers' protocol (BD Biosciences, United Kingdom). An isotype control IgG2bκ (Abcam, Cambridge, United Kingdom) was evaluated for each experimental sample to discriminate the level of background fluorescence of negative cells.

ACCEPTED MANUSCRIPT

ACCEPTED MANUSCRIPT

## 3. Results

### 3.1. DTA0100 inhibits tubulin polymerization by binding to the colchicine site

To analyze the influence of DTA0100 on microtubule formation, we monitored tubulin polymerization by following the absorbance of the solution at 340 nm for 30 min. An increase in absorbance indicated an increase in tubulin polymerization. As positive controls, paclitaxel and colchicine were employed. All the compounds were tested at the same concentration (10 μM) for comparison purposes. As expected, paclitaxel increased the absorbance above the control while colchicine and DTA0100 strongly inhibited microtubule polymerization (Fig. 1B).

To investigate how DTA0100 might bind to the microtubules, we carried out docking experiments of DTA0100 enantiomers. The analysis revealed that both enantiomers bind well at the colchicine binding domain of β-tubulin, with good Gibbs free energy (ΔG) values (-5.6 kcal/mol for both *R* and *S* enantiomers) when compared to colchicine (-8.6 kcal/mol).

As we observed from Fig.1C, the overlap of both enantiomers in the binding site is almost perfect. These docking results confirmed our initial observations that chirality is not a limiting factor on the activity of DTA0100, and enabled us to understand how DTA0100 binds to the colchicine site.

### 3.2. Multi-drug resistant cancer cells have different level of resistance to microtubule targeting agents

The effects of DTA0100 on cancer cell growth were evaluated by the sulforhodamine B assay. The results obtained after 72 h of treatment are shown in Fig. 2. DTA0100 showed significant antiproliferative activity against colorectal carcinoma cell lines reaching GI50values

ACCEPTED MANUSCRIPT

in the nanomolar range. Importantly, DTA0100 was more efficient towards multi-drug resistant colorectal carcinoma cells (Fig. 2A). On the other hand, multi-drug resistant U87-TxR cells were less sensitive to DTA0100 compared to their non-resistant counterparts (Fig. 2B).

Next, we evaluated the sensitivity of DLD1, DLD1-TxR, U87 and U87-TxR cells to various microtubule targeting agents (Table 1). Both multi-drug resistant cancer cell lines demonstrated resistance to microtubule targeting agents including paclitaxel, vinblastine and colchicine. The relative resistance $R_f$ (resistance factor), expressed as the ratio of GI50 concentrations between multi-drug resistant and sensitive cells was used to determine the level of resistance (Table 1). DLD1-TxR exhibited significant resistance to vinblastine ($R_f$ = 20), paclitaxel ($R_f$ = 45) and moderate resistance to colchicine ($R_f$ = 9.1). U87-TxR showed considerable resistance to vinblastine ($R_f$ = 52) and moderate resistance to paclitaxel ($R_f$ = 15) and colchicine ($R_f$ = 6.6). In comparison with aforementioned microtubule targeting agents, DTA0100 activity was not significantly changed in the presence of multi-drug resistant phenotype (Table 1). The GI50 values determined in DLD1 and DLD1- TxR cells were 0.85 μM and 0.45 μM, respectively ($R_f$ = 0.5). The GI50 values obtained in U87 and U87-TxR cells were 4.92 μM and 8.96 μM, respectively ($R_f$= 1.8).

### 3.3. DTA0100 induces apoptosis and cell cycle arrest

The potential of DTA0100 to induce cell death was investigated in DLD1, DLD1-TxR, U87 and U87-TxR cells. After DTA0100 treatment that lasted 72 h, the cells were subjected to AV/PI staining. Flow cytometry analyses revealed cell death-inducing activity of 0.9 μM DTA0100 in DLD1 cells (8.9% of AV+PI- cells in early apoptosis and 16.4% AV+PI+ cells in late apoptosis) in comparison with the untreated control (1.0% of AV+PI- cells in early apoptosis

ACCEPTED MANUSCRIPT

and 3.9% AV+PI+ cells in late apoptosis) (Fig. 3). The percentage of both early and late apoptotic AV+ cells increased from 5.8% in untreated DLD1-TxR cells to 20.8% in those treated with 0.9 μM DTA0100 (Fig. 3). After treatment with 7.5 μM of DTA0100 the percentage of apoptotic AV+ U87 cells increased compared to untreated control (from 9.2% to 26.9%) (Fig. 3). The percentage of apoptotic AV+ cells after treatment of U87-TxR with the same concentration of DTA0100 was also increased but to a lesser extent (from 3.9% in untreated control to 9.6% in DTA0100 treated cells) (Fig. 3). The effect of paclitaxel and colchicine on cell death are presented in Supplemental Fig. 6. The statistical significance of cell death induction by microtubule targeting agents is presented in Supplemental Table 1.

Next, we analyzed the differences in disturbance of cell cycle kinetics after DTA0100 treatment between sensitive and resistant cell lines. Flow cytometry analyses revealed that DTA0100 induced a decrease in $G_1$ phase followed by arrest in S and $G_2$/M phases of cell cycle in DLD1-TxR cells (Fig. 3F).However, the same concentration of compound did not change significantly the cell cycle in corresponding DLD1 cells (Fig. 3E).

Although induced apoptosis (both, early and late) by DTA0100 in DLD1 and DLD1-TxR cell lines was considerably increased 25.3% and 20.8%, respectively, increase in G0 fraction obtained by cell cycle analysis was 4.83% and 9.25%, respectively. This inconsistency can be explained by different sensitivity of applied methodology. Nevertheless, cell cycle pattern in DLD1 treated with DTA0100 showed less prominent change compared to DLD1-TxR.

Treatment with 7.5 μM DTA0100 completely erased the distinctions among cell cycle phases in U87 cells, which is in relation with the increase in the proportion of apoptotic cells (Fig. 3G). In U87-TxR cells, the same concentration of DTA0100 induced a decrease in G1 phase followed by cell cycle arrest in $G_2$/M phase (Fig. 3H).

ACCEPTED MANUSCRIPT

### 3.4. DTA0100 suppresses microtubule network formation

Immunofluorescence staining was performed to investigate the effect of DTA0100 on microtubule network in sensitive and resistant cancer cells. All cell lines were exposed to DTA0100, colchicine and paclitaxel for 24 h at concentrations higher than GI50 values. The images acquired on fluorescent microscope are presented in Fig. 4., while their quantified data are presented in Supplemental Fig. 7. The untreated cells showed typical cytoskeleton structures, with long and dense microtubules extending throughout the cytoplasm. DTA0100 treatment caused destruction of the normal microtubule structure in all cell lines in the same way as the known microtubule destabilizing agent colchicine. Conversely, after treatment with paclitaxel, which is a microtubule stabilizing agent, bundles of microtubules and many abnormal nuclei were observed in all cell lines.

We next addressed whether DTA0100 co-localizes with microtubules and for that purpose we used the DTA0100 less sensitive cell line U87-TxR. Other cell lines were more susceptible to fluorescently labelled DTA0100 (dansyl-DTA0100, Supplemental Fig. 1) and therefore not suitable for the co-localization study. β-tubulin immunostaining was performed after dansyl-DTA0100 labelling of live cells and the images were acquired on a confocal microscope (Fig. 5).

The degree of correlation between β-tubulin and dansyl-DTA0100 was measured using the Pearson correlation coefficient. The obtained coefficient between β-tubulin and dansyl-DTA0100 was 0.417 for U87-TxR cells indicating a positive relationship between β-tubulin and DTA0100.

ACCEPTED MANUSCRIPT

### 3.5. The mRNA expression pattern of Topoisomerase IIα and β-tubulin isoforms in sensitive and multi-drug resistant cells

The expression of the Topoisomerase IIα and β-tubulin isoforms were analyzed from total RNA samples of DLD1, DLD1-TxR, U87 and U87-TxR cells by RT-PCR (Fig. 6A). The expression of Topoisomerase IIα on mRNA level was unaffected by development of multi-drug resistance. The expression of II, III and IVb-β tubulin was increased in U87-TxR cells compared to U87 cells by 2-, 3-, and 1.6-fold, respectively (Fig. 6B). On the other hand, III-β tubulin expression was reduced by 40% in DLD1-TxR cells compared to their sensitive counterparts (Fig. 6B).

### 3.6. Mutational status of *βI-tubulin* gene

In order to determine the mutational status of the *βI-tubulin* gene in sensitive and multi-drug resistant cancer cells, we examined the presence of mutations in the first three exons (1-3) of the *βI-tubulin* gene by DNA sequencing. These experiments showed that sequence of the *βI-tubulin* gene in all tested cancer cell lines did not differ from the wild type sequence.

### 3.7. Influence of DTA0100 on P-glycoprotein activity and expression

To investigate the effect of DTA0100 on P-glycoprotein function in multi-drug resistant cell lines, we analyzed intracellular accumulation of rhodamine 123, which is a P-glycoprotein substrate. The accumulation of rhodamine 123 was assessed by flow-cytometry. Marked increase in rhodamine 123 accumulation was observed in both multi-drug resistant cancer cells lines after treatment with DTA0100, while colchicine did not show the potential to inhibit P-glycoprotein. (Fig. 7A, B). The treatment with DTA0100 led to inhibition of P-glycoprotein function in a

ACCEPTED MANUSCRIPT

concentration - dependent manner, as revealed by the progressive increase in accumulation of rhodamine 123 (Fig. 7C). The effect of DTA0100 on rhodamine 123 accumulation diminished over time (Fig. 7D). However, the GI50 concentration of DTA0100 significantly decreased the expression of P-glycoprotein in both multi-drug resistant cell lines after 72 h (Fig. 7E, F, G).

ACCEPTED MANUSCRIPT

ACCEPTED MANUSCRIPT

## 4. Discussion

Herein, we investigated DTA0100, a propargylic enol ether, with mitotic arrest properties due to its ability to inhibit both Topoisomerase II activity and microtubule network formation. Our previous molecular docking study showed that DTA0100 binds at the binding pocket of the Topoisomerase II α subunit (Silveira-Dorta et al., 2013). Considering DTA0100 strong ability to induce mitotic arrest in many different cell lines (Leon et al., 2010), we decided to explore its effect on tubulin polymerization. Indeed, DTA0100 inhibited tubulin polymerization *in vitro* in the same manner as colchicine, a well-konwn microtubule destabilizing agent. Next, we verified by molecular docking study that DTA0100 binds on microtubule at colchicine site.

It is known that the efficacy of microtubule targeting agents is compromised by the emergence of drug resistance due to the changes in β-tubulin isoforms' expression and/or mutations and P-glycoprotein overexpression. Therefore, this study was aimed to reveal the possible interactions of DTA0100 with microtubule network and P-glycoprotein in multi-drug resistant cancer cells. To that end, we employed two pairs of sensitive and multi-drug resistant cancer cell lines (human colorectal carcinoma and glioblastoma cells). Both multi-drug resistant cancer cell lines were developed by continuous exposure to paclitaxel and both lines are characterized by significantly increased P-glycoprotein expression and activity (Podolski-Renić et al., 2013).

Besides paclitaxel, we found that the cytotoxicity of other microtubule targeting agents, vinblastine and colchicine was also decreased in both multi-drug resistant cancer cell lines. Nevertheless, multi-drug resistant colorectal carcinoma cells were more sensitive towards DTA0100, while the presence of resistant phenotype in U87-TxR cell line only slightly decreased the inhibitory potential of DTA0100 compared to other microtubule interacting agents.

ACCEPTED MANUSCRIPT

Afterwards, we tested the effects of DTA0100 on cell death induction and cell cycle distribution. DTA0100 induced apoptosis in both colorectal carcinoma cell lines with the similar efficacy, but the effect on cell cycle kinetics was more prominent in multi-drug resistant colorectal carcinoma cells. While DTA0100 induced a decrease in $G_1$ phase followed by arrest in S and $G_2$/M phase of the cell cycle in DLD1-TxR cells, the same concentration of compound did not affect significantly the cell cycle in corresponding DLD1 cells. DTA0100's effect on apoptosis induction was more prominent in U87 cells compared to their resistant counterparts. In addition, DTA0100 devastated cell cycle distribution by completely erasing the distinctions among cell cycle phases in U87 cells. The cell cycle arrest at $G_2$/M phase in U87-TxR cells was caused by the same concentration of this compound confirming its anti-mitotic effect. This is in accordance with previous report showing that DTA0100 induced cell cycle perturbation and $G_2$/M arrest (León et al., 2010).

Knowing that increased P-glycoprotein expression is present in both multi-drug resistant cancer models, we assumed that some other mechanisms altered during the acquisition of resistant phenotype rather than P-glycoprotein may confer different sensitivity to DTA0100. There is a wide range of cellular alterations acquired during development of multi-drug resistance: diminished response to apoptotic signaling, up-regulated DNA damage repair mechanisms, altered drug targets, and enhanced drug detoxification (Kachalaki et al., 2016). Since both multi-drug resistant cancer cell lines were established after continuous treatment with paclitaxel, the rational assumption was that changes in β-tubulin provoked by exposure to paclitaxel could affect efficiency of DTA0100.

To that end, we analyzed the effect of DTA0100 on the microtubule network in sensitive and multi-drug resistant cancer cells. By fluorescent microscopy, we showed extensive

ACCEPTED MANUSCRIPT

disruption of the microtubule cytoskeleton in all cell lines after treatment with DTA0100. We compared the effect of DTA0100 with colchicine and paclitaxel and observed the similarity with microtubule destabilizing agent - colchicine. A destabilizing effect on microtubules was further verified by confocal microscopy. Importantly, dansyl-DTA0100 colocalised with β-tubulin in U87-TxR cells, confirming the interaction of DTA0100 with β-tubulin.

Accordingly, we assumed that potential changes in Topoisomerase IIα and β-tubulin developed during resistance induction by paclitaxel may interfere with DTA0100 activity. The expression pattern of Topoisomerase IIα mRNA was not changed between sensitive and multi-drug resistant cell lines. Further, we analyzed the presence of mutations in *βI-tubulin* gene and the level of expression of the β-tubulin isoforms. Mutations in *βI-tubulin* gene were not found in both multi-drug resistant cancer models. The expression of βII-, βIII- and βIVb-tubulin mRNAs was increased in U87-TxR cells, while the class III was decreased in DLD-TxR cells. Previous studies using siRNA approaches showed that βIII-tubulin silencing increases sensitivity to paclitaxel and *Vinca* alkaloids in non-small cell lung carcinoma (Kavallaris et al., 1999) and breast carcinoma cells (Stengel et al., 2009). In agreement with this, stable overexpression of βIII-tubulin was found to correlate with lower sensitivity to paclitaxel, docetaxel, epothilone B and vinblastine in HeLa cells (Risinger et al., 2008). The findings that βIII-tubulin expression is critical for the sensitivity of both stabilizing and destabilizing microtubule targeting agents underscore the importance of this isoform in the development of drug resistance. Hence, our results showed increased sensitivity of multi-drug resistant colorectal carcinoma cells to DTA0100 that partly could be explained with decreased expression of the βIII-tubulin isoform. Significantly increased sensitivity to *Vinca* alkaloids (Gan and Kavallaris, 2008) and epotilone B (Gan et al., 2011) was observed after silencing of other isoforms βII- and βIVb-tubulin.

ACCEPTED MANUSCRIPT

Therefore, reduced sensitivity of multi-drug resistant glioma cells to DTA0100 could be explained by the increased expression of βII-, βIII- and βIVb-tubulin mRNAs. It is possible that increased expression of βII-, βIII- and βIVb-tubulin may affect the dynamic nature of the microtubules (Huzil et al, 2007; Orr et al., 2003) and change the accessibility of DTA0100 to its binding-site leading to impaired efficacy of this compound in multi-drug resistant glioma cells. Moreover, increased expression of these β-tubulin isoforms may influence the interactions of microtubules with other components of the cytoskeleton (Gan et al., 2007; Nogales et al., 2000) and hence affect cellular response to DTA0100.

Since our results showed selectivity of DTA0100 against multi-drug resistant colorectal carcinoma cells with P-glycoprotein overexpression, we assumed that this compound is unlikely to be P-glycoprotein substrate such as paclitaxel, vinblastine and colchicine (Bikadi et al., 2011; Wang et al., 2005). Moreover, DTA0100 decreased the activity of P-glycoprotein pump in a dose-dependent manner as we verified by increased accumulation of rhodamine 123 in both resistant cancer cell lines. These results suggest that DTA0100 may be used as P-glycoprotein inhibitor. However, the efficacy of DTA0100 against P-glycoprotein activity declined over time. Therefore, we tested its influence on P-glycoprotein expression after 72 h and found that DTA0100 did not increase the P-glycoprotein expression. Quite opposite to other Topoisomerase IIα inhibitors and microtubule interacting agents, DTA0100 was able to decrease the P-glycoprotein expression. Recently, YCH337, a novel α-carboline derivative was reported to target both microtubule and Topisomerase II with a potential to overcome the drug resistance problem (Yi et al., 2015). Although with unrelated chemical structure, YCH337 and DTA0100 share similar anticancer properties as well as similar pattern of action against multi-drug resistant

ACCEPTED MANUSCRIPT

cells. Therefore, these drugs offer a unique strategy that may abrogate the application of two or more drugs in cancer treatment.

## 5. Conclusions

The identification of new anticancer drugs which activity could not be diminished by developed multi-drug resistance mechanisms is emerging. Herein, we verified that DTA0100 possesses featured characteristics of an anticancer agent. It acts as an inhibitor of both Topoisomerase IIα and microtubule network formation. Importantly, DTA0100 efficacy is not significantly changed in cells with the overexpression of P-glycoprotein. Contrary, DTA0100 is able to suppress P-glycoprotein activity without inducing its expression. The mechanisms which DTA0100 targets usually provide selective advantage to resistant cancer cells making them less sensitive to many drug types including drugs that are P-glycoprotein substrates. The sensitivity of both multi-drug resistant cell lines was not compromised by DTA0100 treatment as it is in the case with Topoisomerase IIα inhibitors and microtubule targeting agents. Therefore, DTA0100 could be considered as a new anticancer agent able to overcome problems in the therapeutic approaches with microtubule targeting agents. Its straightforward synthesis (León, et al., 2010) makes this drug appealing for massive production and wide application in malignancies.

ACCEPTED MANUSCRIPT

ACCEPTED MANUSCRIPT

## Acknowledgements

The authors acknowledge the support from the Ministry of Education, Science and Technological Development of the Republic of Serbia (Grant No III41031), the EU Research Potential (FP7-REGPOT- 2012-CT2012-31637-IMBRAIN), the European Regional Development Fund (FEDER) and the Spanish MINECO (CTQ2014-56362- C2-1- P). This work was performed within the framework of COST Action CM1407 (Challenging organic syntheses inspired by nature - from natural products chemistry to drug discovery).

## Conflict of interest

The authors declare that they have no conflict of interest.

## References

Bailly, C., 2012. Contemporary challenges in the design of topoisomerase II inhibitors for cancer chemotherapy. Chem. Rev. 112, 3611-3640.

Beck, W., Morgan, S., Mo, Y., Bhat U., 1999. Tumor cell resistance to DNA topoisomerase II inhibitors: new developments. Drug Resist. Updat. 2, 382-389.

Bikadi, Z., Hazai, I., Malik, D., Jemnitz, K., Veres, Z., Hari, P., Ni, Z., Loo, T. W., Clarke, D. M., Hazai, E., Mao, Q., 2011. Predicting P-glycoprotein-mediated drug transport based on support vector machine and three-dimensional crystal structure of P-glycoprotein. PLoS One 6, e25815.

Ferguson, R. E., Taylor, C., Stanley, A., Butler, E., Joyce, A., Harnden, P., Patel, P. M., Selby, P. J., Banks, R. E., 2005. Resistance to the tubulin-binding agents in renal cell carcinoma: no mutations in the class I beta-tubulin gene but changes in tubulin isotype protein expression. Clin. Cancer Res. 11, 3439-3445.

Gan, P. P., Pasquier, E., Kavallaris, M., 2007. Class III beta-tubulin mediates sensitivity to chemotherapeutic drugs in non small cell lung cancer. Cancer Res. 67, 9356-9363.

Gan, P. P., Kavallaris M., 2008. Tubulin-targeted drug action: functional significance of class II and class IVb beta-tubulin in vinca alkaloid sensitivity. Cancer Res. Dec. 68, 9817-9824.

ACCEPTED MANUSCRIPT

Gan, P. P., McCarroll, J. A., Byrne, F. L., Garner, J., Kavallaris, M., 2011. Specific β-tubulin isotypes can functionally enhance or diminish epothilone B sensitivity in non-small cell lung cancer cells. PLoS One 6, e21717.

Ganapathi, R., Ganapathi, M., 2013. Mechanisms regulating resistance to inhibitors of topoisomerase II. Front. Pharmacol. 4, 89.

Hande, K., 2008. Topoisomerase II inhibitors. Update Cancer Ther. 3, 13-26.

Huzil, J. T., Chen, K., Kurgan, L., Tuszynski, J. A., 2007. The roles of beta-tubulin mutations and isotype expression in acquired drug resistance. Cancer Inform. 3, 159-181.

Jordan, M. A., Wilson, L., 2004. Microtubules as a target for anticancer drugs. Nat. Rev. Cancer 4, 253-265.

Kachalaki, S., Ebrahimi, M., Mohamed Khosroshahi, L., Mohammadinejad, S., Baradaran, B., 2016. Cancer chemoresistance; biochemical and molecular aspects: a brief overview. Eur. J. Pharm. Sci. 89, 20-30.

Kavallaris, M., Burkhart, C. A., Horwitz, S. B., 1999. Antisense oligonucleotides to class III beta-tubulin sensitize drug-resistant cells to Taxol. Br. J. Cancer 80, 1020-1025.

Leandro-García, L. J., Leskelä, S., Landa, I., Montero-Conde, C., López-Jiménez, E., Letón, R., Cascón, A., Robledo, M., Rodríguez-Antona, C., 2010. Tumoral and tissue-specific expression of the major human beta-tubulin isotypes,. Cytoskeleton 67, 214-223

León, L. G., Ríos-Luci, C., Tejedor, D., Pérez-Roth, E., Montero, J. C., Pandiella, A., García-Tellado, F., Padrón, J. M., 2010. Mitotic arrest induced by a novel family of DNA topoisomerase II inhibitors. J. Med. Chem. 53, 3835-3839.

Manders, E. M., Stap, J., Brakenhoff, G. J., van Driel, R., Aten, J. A., 1992. Dynamics of three-dimensional replication patterns during the S-phase, analysed by double labelling of DNA and confocal microscopy. J. Cell. Sci. 103, 857-862.

Manders, E. M., Verbeek, F. J., Aten, J. A., 1993. Measurement of co-localization of objects in dual-colour confocal images. J. Microsc. 169, 375-382.

.

McGrogan, B. T., Gilmartin, B., Carney, D. N., McCann, A., 2008. Taxanes, microtubules and chemoresistant breast cancer. Biochim. Biophys. Acta 1785, 96-132.

McCloy, R. A., Rogers, S., Caldon, C. E., Lorca, T., Castro, A., Burgess, A., 2014. Partial inhibition of Cdk1 in G 2 phase overrides the SAC and decouples mitotic events. Cell Cycle 13, 1400-1412.

ACCEPTED MANUSCRIPT

Nogales, E., 2000. Structural Insights into Microtubule Function, Annu. Rev. of Biochem. 69, 277-302.

Orr, G. A., Verdier-Pinard, P., McDaid, H., Horwitz, S. B., 2003. Mechanisms of Taxol resistance related to microtubules. Oncogene 22, 7280-7295.

Podolski-Renić, A., Andelković, T., Banković, J., Tanić, N., Ruždijić, S., Pešić, M., 2011. The role of paclitaxel in the development and treatment of multidrug resistant cancer cell lines. Biomed. Pharmacother. 65, 345-353.

Podolski-Renić, A., Jadranin, M., Stanković, T., Banković, J., Stojković, S., Chiourea, M., Aljančić, I., Vajs, V., Tešević, V., Ruždijić, S., Gagos, S., Tanić, N., Pešić, M., 2013. Molecular and cytogenetic changes in multi-drug resistant cancer cells and their influence on new compounds testing. Cancer Chemother. Pharmacol. 72, 683-697.

Ponte, P., Ng, S., Engel, J., Gunning, P., Kedes, L., 1984. Evolutionary conservation in the untranslated regions of actin mRNAs: DNA sequence of a human betaactin cDNA. Nucleic Acids Res. 12, 1687-1696.

Riordan, J. R., Ling, V., 1985. Genetic and biochemical characterization of multidrug resistance. Pharmacol. Ther. 28, 51-75.

Risinger, A. L., Jackson, E. M., Polin, L. A., Helms, G. L., LeBoeuf, D. A., Joe, P. A., Hopper-Borge, E., Ludueña, R. F., Kruh, G. D., Mooberry, S. L., 2008. The taccalonolides: microtubule stabilizers that circumvent clinically relevant taxane resistance mechanisms. Cancer Res. 68, 8881-8888.

Shalli, K., Brown, I., Heys, S. D., Schofield, A. C., 2005. Alterations of beta-tubulin isotypes in breast cancer cells resistant to docetaxel. FASEB J. 19, 1299-1301.

Sharom, F., 2008. ABC multidrug transporters: structure, function and role in chemoresistance. Pharmacogenomics 9, 105-127.

Silveira-Dorta, G., Sousa, I. J., Ríos-Luci, C., Martín, V. S., Fernandes, M. X., Padrón, J. M., 2013. Molecular docking studies of the interaction between propargylic enol ethers and human DNA topoisomerase IIα. Bioorg. Med. Chem. Lett. 23, 5382-5384.

Stengel, C., Newman, S. P., Leese, M. P., Potter, B. V., Reed, M. J., Purohit, A., 2009. Class III beta-tubulin expression and in vitro resistance to microtubule targeting agents. Br. J. Cancer 102, 316-324.

Wang, Y. H., Li, Y., Yang, S. L., Yang, L., 2005. Classification of substrates and inhibitors of P-glycoprotein using unsupervised machine learning approach. J. Chem. Inf. Model 45, 750-757.

Wong, H., Anderson, W. D., Cheng, T., Riabowol, K. T., 1994. Monitoring mRNA expression by polymerase chain reaction: the "primer-dropping" method. Anal. Biochem. 223, 251-258.

ACCEPTED MANUSCRIPT

Yi, JM., Zhang XF., Huan XJ., Song SS., Wang W., Tian QT., Sun YM., Chen Y., Ding J., Wang YQ., Yang CH., Miao ZH., 2015. Dual targeting of microtubule and topoisomerase II by α-carboline derivative YCH337 for tumor proliferation and growth inhibition. Oncotarget 6, 8960-8973.

ACCEPTED MANUSCRIPT

ACCEPTED MANUSCRIPT

## Figure Legends

**Fig. 1.** DTA0100 inhibits *in vitro* tubulin assembly by binding to the colchicine site. (**A**) Chemical structure of DTA0100. (**B**) Tubulin was polymerized for 30 min at 37 °C in the presence of 10 μM of paclitaxel, colchicine and DTA0100, and the absorbance at 340 nm was monitored. (**C**) Comparison of (*R*)-DTA0100 (yellow) and (*S*)-DTA0100 (green) conformations docked at the colchicine binding site of β-tubulin.

**Fig. 2.** Cell growth inhibition by DTA0100. (**A**) Dose-dependent cell growth inhibition of DLD1 and DLD1-TxR, (**B**) U87 and U87-TxR assessed by the sulforhodamine B assay after 72 h of DTA0100 treatment. The average ± SD was obtained from five independent experiments (n=5). The results were considered to be statistically significant when $p< 0.05$ (*); $p< 0.001$ (***).

**Fig. 3.** Cell death induction and changes in cell cycle distribution after treatment with DTA0100. Cell death and modulations in cell cycle kinetics were assessed by flow cytometry. DLD1 and DLD1-TxR cells were treated for 72 h with 0.9 μM of DTA0100, while U87 and U87-TxR cells were treated with 7.5 μM of DTA0100. Cells were stained with AV/ PI to detect the presence of cell death. Flow-cytometric assay distinguishes viable (AV- PI-), early apoptotic (AV+ PI-), late apoptotic (AV+ PI+) and necrotic (AV- PI+) cells. Cell cycle analysis was performed by FACScalibur flow-cytometry, using Mod-FIT software. Again, DLD1 and DLD1-TxR cells were treated for 72 h with 0.9 μM of DTA0100, while U87 and U87-TxR cells were treated with 7.5 μM of DTA0100. Y-axis: relative cell numbers. X-axis: DNA content by propidium iodide. The percent of cells in G0, G1, S and G2/M phases are from three representative experiments. The

ACCEPTED MANUSCRIPT

arrows indicate particular change induced by DTA0100 concerning increase (↑) and decrease (↓) in the percentage of cells distributed in cell cycle phases.

**Fig. 4.** DTA0100 suppresses microtubule polymerization. DLD1, DLD1-TxR, U87 and U87-TxR cells were treated for 24 h with DTA0100, colchicine and paclitaxel at concentrations close to GI50. Microtubules were labeled with β-tubulin antibody (green). Nuclei were counterstained with Hoechst 33342 (blue). Scale bar = 20 μm.

**Fig. 5.**Co-localization of DTA0100 with β-tubulin. U87-TxR cells were labelled with β-tubulin antibody (green) and dansyl-DTA0100 (red). Scale bar = 20 μm.

**Fig. 6.** RT-PCR analysis of Topoisomerase IIα and β-tubulin isoforms expression. The mRNA expression of (**A**) Topoisomerase IIα and (**B**) β-tubulin isoforms was normalized to the internal control (β-actin or gapdh). The samples were loaded on agarose gel next to 100 bp DNA ladder. The relative expression was calculated as a relation between expressions of mRNAs of interest and internal control. The average ± SD was obtained from five independent experiments (n=5). Statistical significance is presented as: $p<0.05$ (*), $p<0.01$ (**), $p<0.001$ (***).

**Fig. 7.** DTA0100 inhibits P-glycoprotein function in a dose-dependent and time-dependent manner and decreases the expression of P-glycoprotein. (**A**) Flow cytometric profile of rhodamine 123 accumulations in DLD1, DLD1-TxR, U87 and U87-TxR cells. Multi-drug resistant cells were treated with 10 μM of either DTA0100 or colchicine. Two independent experiments were performed (a minimum of 10,000 events were collected for each experimental

ACCEPTED MANUSCRIPT

sample). (**B**) Comparison between DTA0100 and colchicine effect on rhodamine 123 accumulation in multi-drug resistant cells. (**C**) Analysis of rhodamine 123 accumulation after application of different DTA0100 concentrations. (**D**) The effect of DTA0100 on rhodamine 123 accumulation over time. (**E**) Flow-cytometric profiles of P-glycoprotein expression in DLD1 and DLD1-TxR cells. DLD1-TxR cells were treated with DTA0100. Dashed lines represent negative controls. Two independent experiments were performed (a minimum of 10,000 events were collected for each experimental sample). Analysis of P-glycoprotein expression after 72 h in (**F**) DLD1-TxR cells treated with 0.9 μM DTA0100 and (**G**) U87-TxR cells treated with 7.5 μM DTA0100. Statistical significance between sensitive and multi-drug resistant cancer cells: $p < 0.001$ (***). Statistical significance between untreated and treated multi-drug resistant cells: $p < 0.01$ (##), $p < 0.001$ (###). Statistical significance between different treatments: $p < 0.001$ ($$$).

ACCEPTED MANUSCRIPT

ACCEPTED MANUSCRIPT

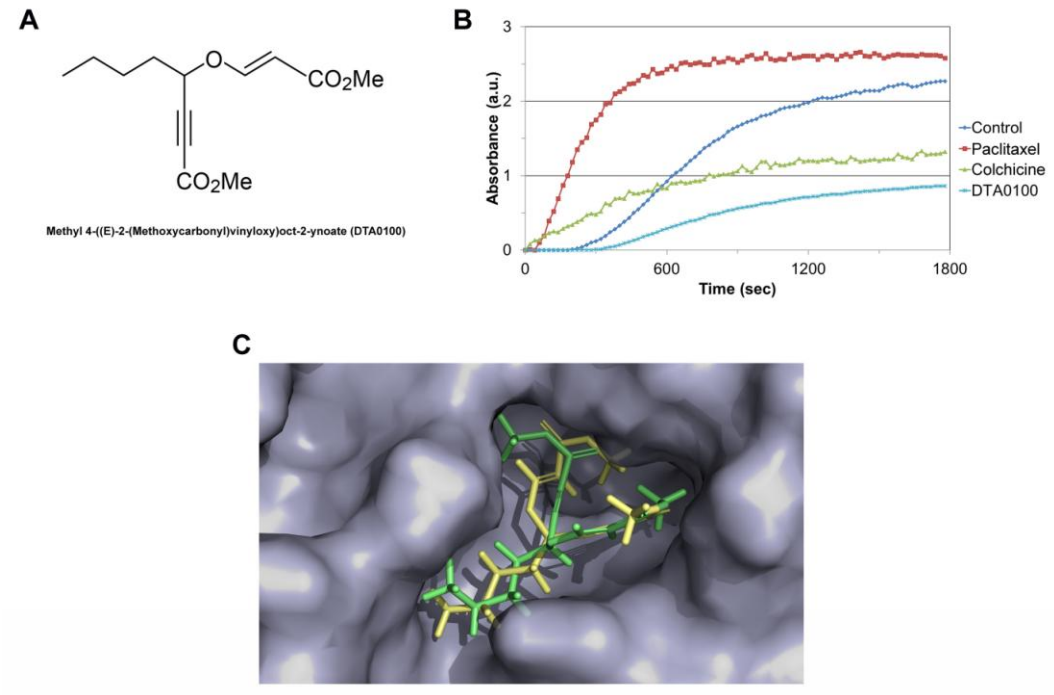


Figure 1

ACCEPTED MANUSCRIPT

ACCEPTED MANUSCRIPT

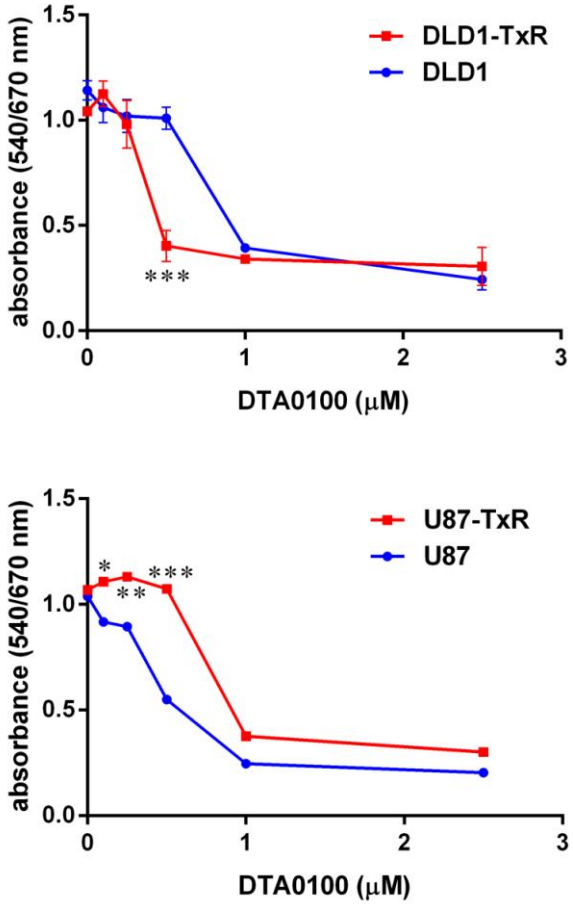


Figure 2

ACCEPTED MANUSCRIPT

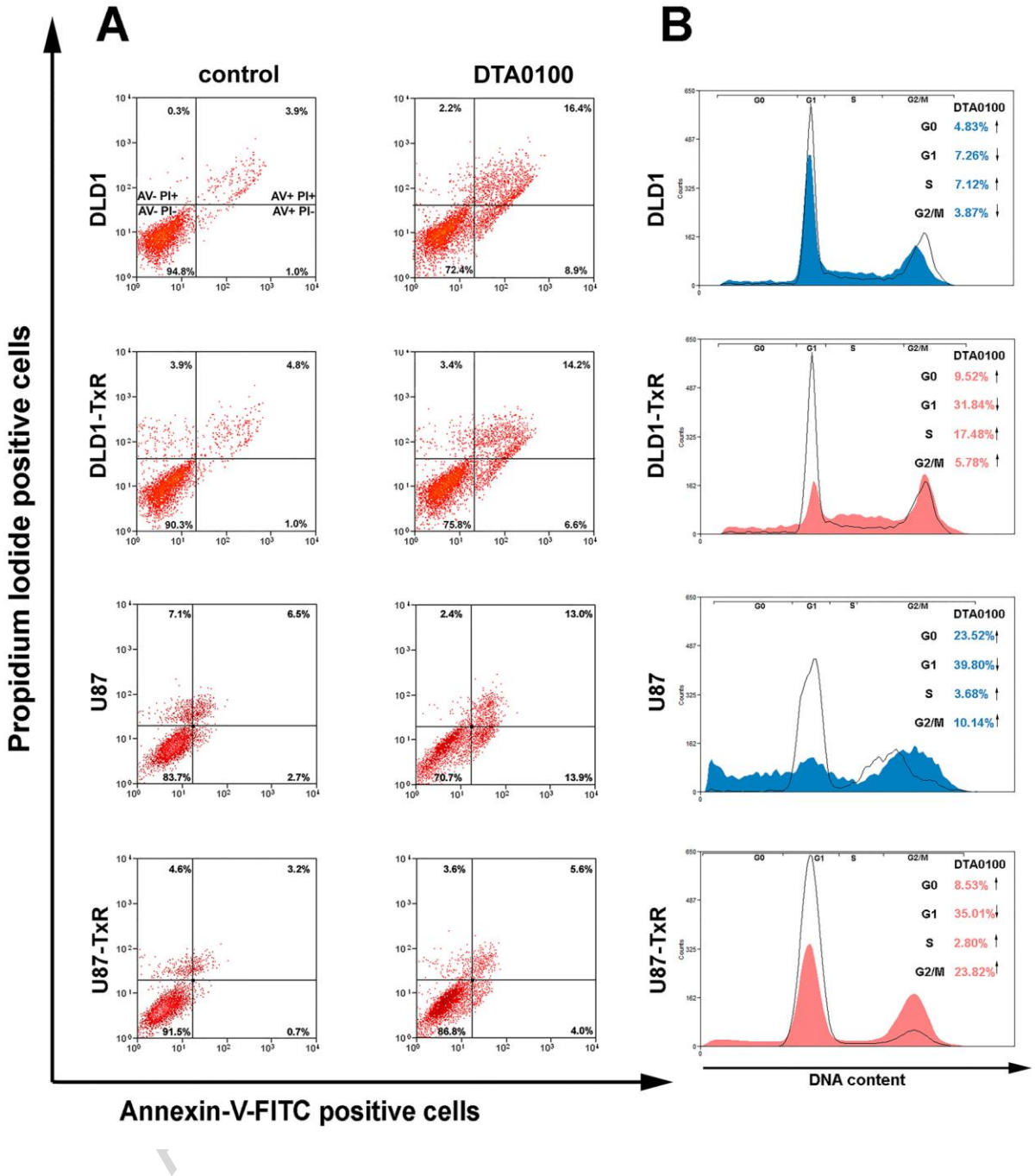


Figure 3

ACCEPTED MANUSCRIPT

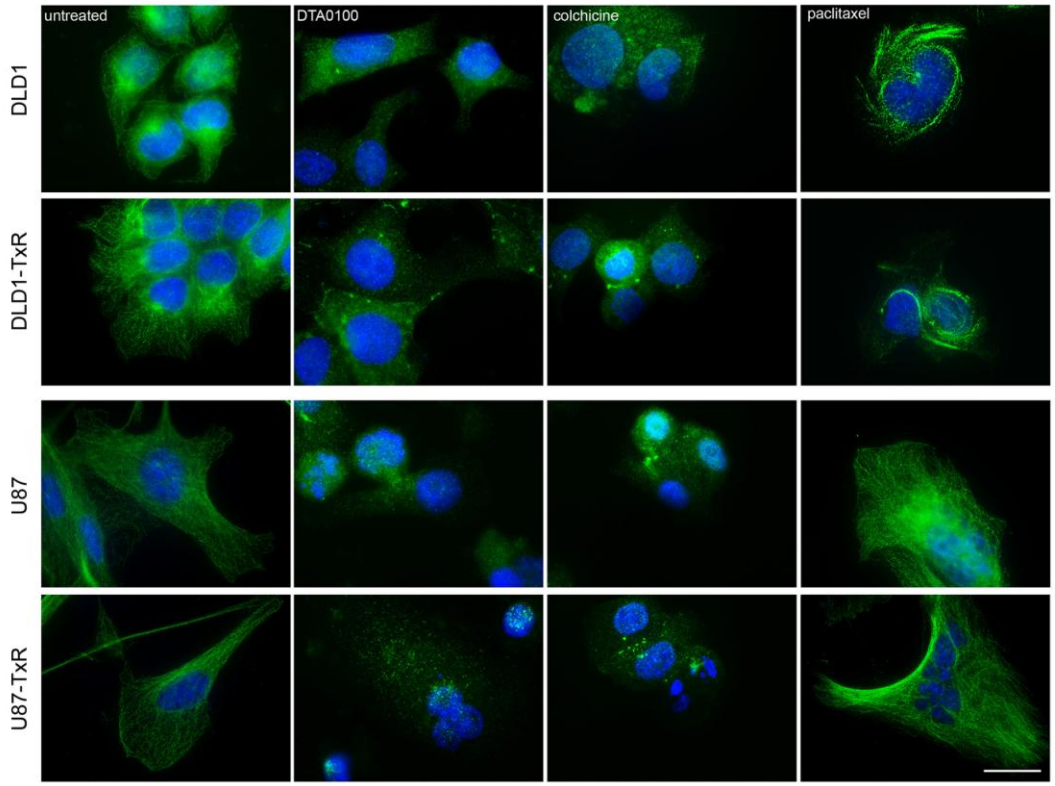


Figure 4

ACCEPTED MANUSCRIPT

ACCEPTED MANUSCRIPT

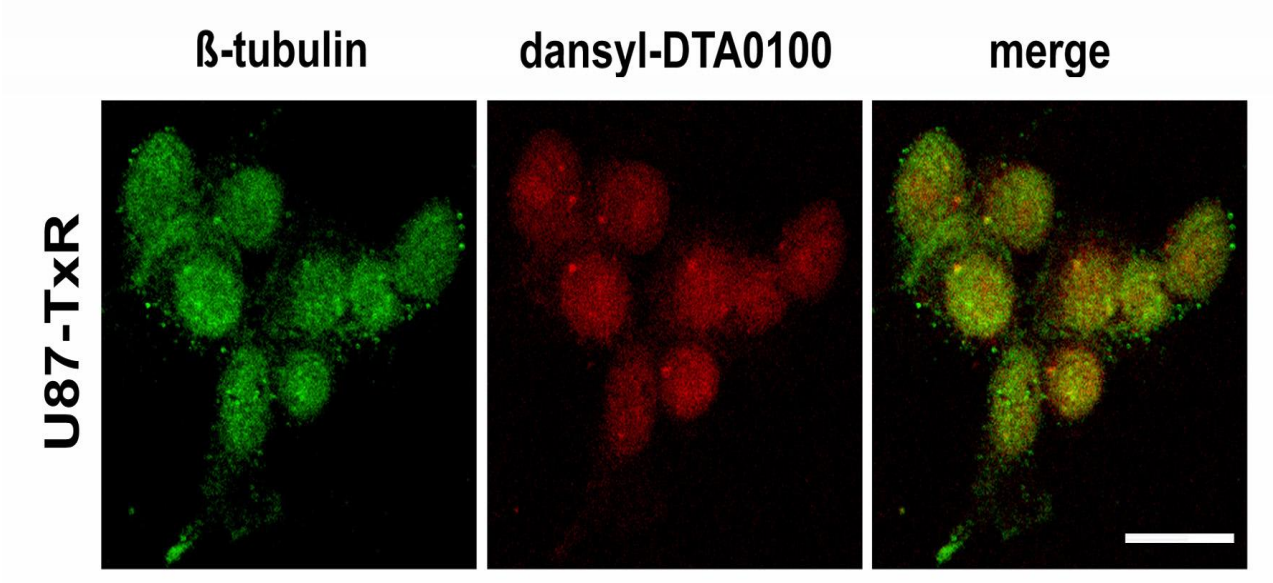


Figure 5

ACCEPTED MANUS

ACCEPTED MANUSCRIPT

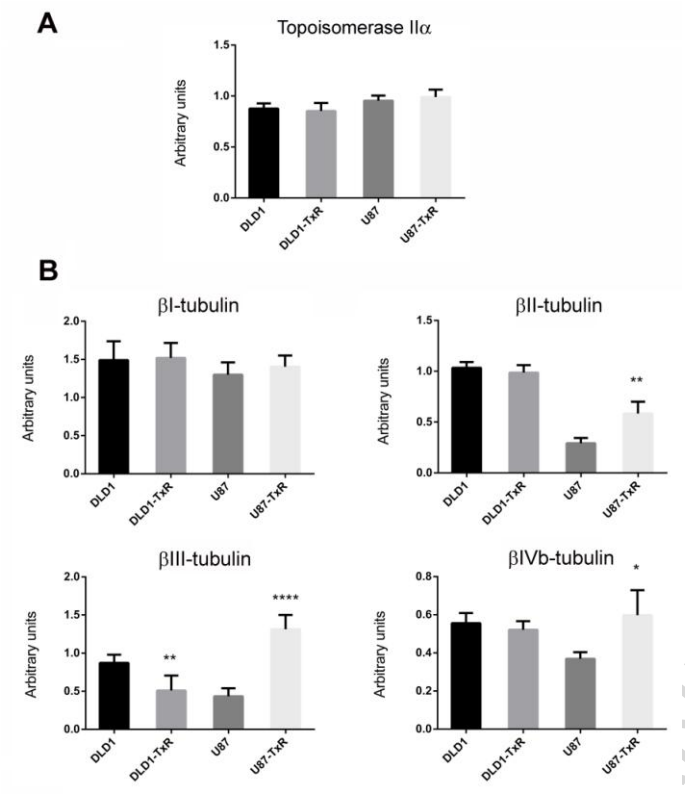


Figure 6

ACCEPTED MANUSCRIPT

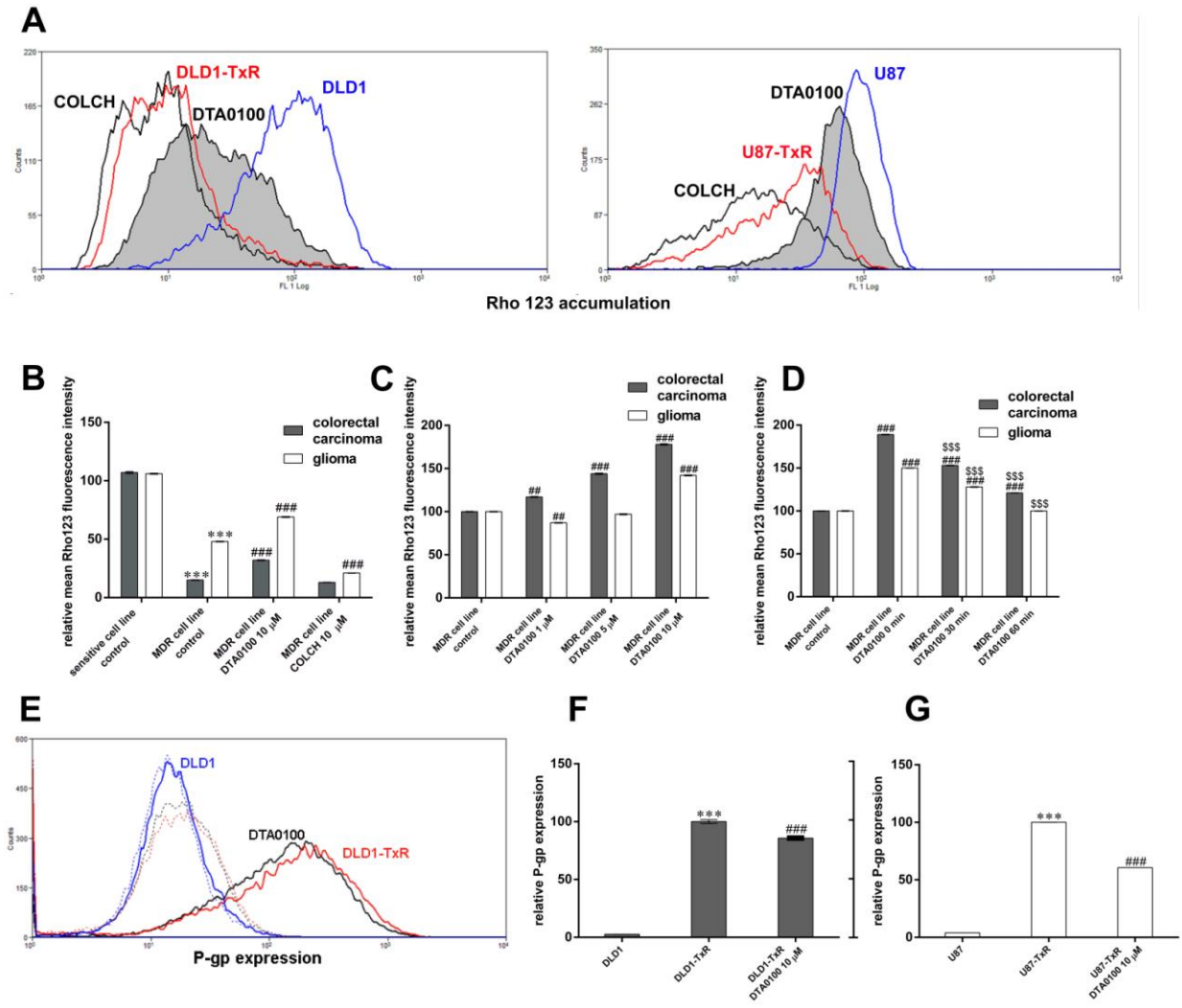


Figure 7

ACCEPTED MANUSCRIPT

**Table 1.** Cross-resistance profile to various microtubule targeting agents obtained by sulforhodamine B assay

| Drugs | $GI_{50}$ (µM)[a] | | Rf[b] | $GI_{50}$ (µM)[a] | | Rf[c] |
|---|---|---|---|---|---|---|
| | DLD1 | DLD1-TxR | | U87 | U87 TxR | |
| DTA0100 | 0.85 | 0.45 | 0.5 | 4.92 | 8.96 | 1.8 |
| Colchicine | 0.02 | 0.17 | 9.1 | 0.02 | 0.13 | 6.6 |
| Vinblastine | 0.01 | 0.2 | 20 | 0.006 | 0.31 | 52 |
| Paclitaxel | 0.04 | 1.81 | 45 | 0.09 | 1.33 | 15 |

[a]Values represent the average from three independent experiments. GI50 was calculated by nonlinear regression analysis using GraphPad Prism 6.
[b]Relative resistance of DLD1-TxR to DLD1
[c]Relative resistance of U87-TxR to U87

ACCEPTED MANUSCRIPT

ACCEPTED MANUSCRIPT

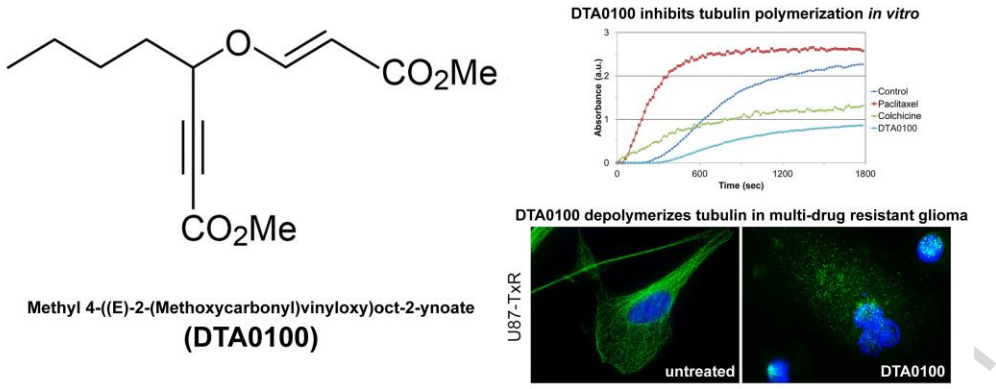


Graphical abstract